

Article

**Demonstration of Electrochemical Generation of  
Solution-Phase Hot Electrons at Oxide-Covered Tantalum  
Electrodes by Direct Electrogenenerated Chemiluminescence**

Yung-Eun Sung, Frdric Gaillard, and Allen J. Bard

*J. Phys. Chem. B*, **1998**, 102 (49), 9797-9805 • DOI: 10.1021/jp981985y

Downloaded from <http://pubs.acs.org> on January 23, 2009

**More About This Article**

---

Additional resources and features associated with this article are available within the HTML version:

- Supporting Information
- Links to the 1 articles that cite this article, as of the time of this article download
- Access to high resolution figures
- Links to articles and content related to this article
- Copyright permission to reproduce figures and/or text from this article

[View the Full Text HTML](#)



**ACS Publications**  
High quality. High impact.

# Demonstration of Electrochemical Generation of Solution-Phase Hot Electrons at Oxide-Covered Tantalum Electrodes by Direct Electrogenerated Chemiluminescence

Yung-Eun Sung,<sup>†</sup> Frédéric Gaillard, and Allen J. Bard\*

Department of Chemistry and Biochemistry, The University of Texas at Austin, Austin, Texas 78712

Received: April 24, 1998; In Final Form: October 10, 1998

Experimental evidence for the production of hot electrons in an acetonitrile solution from a Ta<sub>2</sub>O<sub>5</sub>-covered Ta electrode was provided by electrogenerated chemiluminescence (ECL) and electrochemical measurements. Electron transfer to solution species occurred via the Ta<sub>2</sub>O<sub>5</sub> conduction band, as demonstrated by comparative measurements with a number of one-electron redox couples at Pt and Ta electrodes. The oxidized forms of thianthrene and a heptamethine cyanine dye were selected as the species capable of direct formation of the excited state and ECL upon hot electron injection. The observation of ECL emission upon a cathodic potential step (a process that does not occur at a metal electrode) confirmed the occurrence of this process. ECL emission at Ta/Ta<sub>2</sub>O<sub>5</sub> was also observed during reduction of Ru(bpy)<sub>3</sub><sup>3+</sup> (bpy = bipyridine). Reasons for the low efficiency of the ECL process via hot electrons at the metal/metal oxide/solution interface are discussed.

## Introduction

This paper deals with electrochemical processes involving hot electrons in the solution phase. Hot electrons are defined as electrons with thermal energies ( $kT_h$ ) greater than the thermal energy ( $kT$ ) of a phase<sup>1</sup> or as electrons at an energy far above the Fermi energy of a phase.<sup>2</sup> Hot electrons have been studied in metals, semiconductors, and liquids. Hot electrons in the metal phase ( $e_h^m$ ) can be produced by irradiation of the electrode. Although electrons in a metal relax to the equilibrium Fermi level on a time scale of 10–1000 fs,<sup>3</sup> those formed within the mean free path of a metal/solution interface ( $\sim 50$ – $100$  nm) can be injected into the solution to form a hot electron in that phase ( $e_h^s$ ) (Figure 1A).<sup>4,5</sup> There have also been studies of hot electrons in semiconductors. In a semiconductor, hot electrons are those with energies appreciably higher than the conduction band edge. Of interest in these latter studies is the injection of electrons into the solution phase that are hot in the semiconductor and are produced by irradiation with photons of energies larger than the semiconductor band gap, before they thermalize to the conduction band edge energy in the semiconductor.<sup>6–8</sup> The process of injection of hot electrons from the semiconductor into solution has been examined by noting the occurrence of chemical reactions in solution that would not be possible with thermalized semiconductor electrons. However, as noted recently, measurements of this type are experimentally challenging because one must ensure that shifts of the semiconductor Fermi level do not occur during the irradiation step.<sup>9</sup>

Hot electrons in the liquid phase can be produced by high-energy radiation, photoionization, or injection from an electrode.<sup>1</sup> The relaxation time for the hot electron to thermalize ( $e_h^h \rightarrow e_t^s$ ) depends on the nature of the liquid and ranges from nanoseconds for liquid Xe and Kr to the picosecond regime for molecular liquids. The thermalized electron can form a solvated electron in the medium or react directly with a solution species. In the studies reported here, we are interested in the production of hot electrons in solution, without irradiation, by the applica-

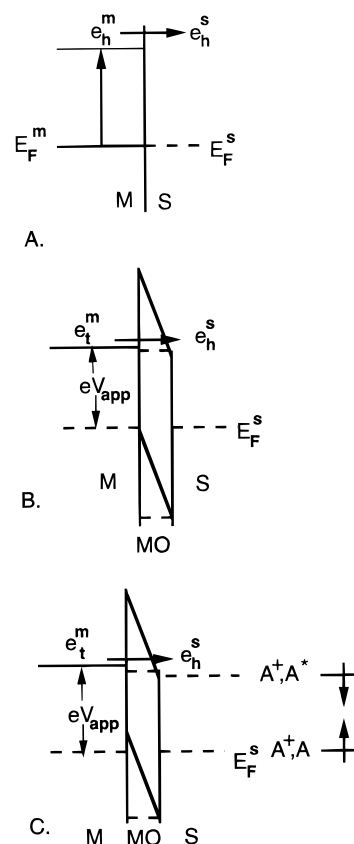


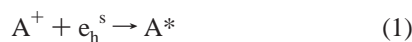
**Figure 1.** Schematic diagram of (A) photoinjection of hot electrons into solution from metal and dark injection (B) through metal/metal oxide interface and (C) with production of an excited state in solution. The Fermi level in solution,  $E_F^s$  is governed by the redox couple  $A^+/A$ .

tion of an electric field across a metal/metal oxide interface (Figure 1B). In this case, a layer of metal oxide (MO) with a large band gap, e.g., Ta<sub>2</sub>O<sub>5</sub>, prevents electron transfer from the metal to a solution species until a large electric field exists across the oxide and the Fermi level in the metal is above that of the

<sup>†</sup> Current address: Department of Materials Science & Engineering, Kwangju Institute of Science and Technology, Kwangju 506-712, S. Korea.

conduction band of the metal oxide. Current flow across the oxide film can then produce a hot solution-phase electron ( $e_{\text{h}}^{\text{m}} \rightarrow e_{\text{h}}^{\text{s}}$ ). Production of hot solution-phase electrons need not involve electrons that are hot in the oxide phase as long as the conduction band edge is above the Fermi level in the solution at the electrode surface. This solution Fermi level is equivalent to the electrochemical potential of an equilibrium electron in the solution,  $\bar{\mu}_{\text{e}}^{\text{s}}$ , and is governed by the redox couples in the medium or more precisely by the  $E^{\circ}$ 's and the ratio of the oxidized and reduced forms at the electrode surface. An experiment of this type, with an M/MO/M' structure ( $M = \text{Al}$  or  $\text{Mg}$  and  $M' = \text{Ag}$ ) was recently described by Diesing et al.<sup>10</sup> These authors produced hot electrons in the Ag solution contact by adding a tunneling bias between the Al or Mg and Ag and identified hot-electron processes in an aqueous acetate buffer by examination of the current–potential curves for the hydrogen evolution reaction. In similar experiments with an n-Si/Au structure, hot-electrons were injected to reduce  $\text{Fe}(\text{CN})_6^{3-}$  where the hot-electron effects were identified on the basis of the effect of the Au film thickness on the measured exchange current.<sup>11</sup>

Our approach to demonstrate solution-phase hot electron production is through the formation of an excited state in solution (Figure 1C). In this experiment, the solution contains an oxidized species,  $A^+$ , which is capable of forming an excited state,  $A^*$ , upon reduction at potential  $E_{\text{c}}$ :



where  $E_{\text{c}} + E^{\circ}(A^+, A)$  is greater than the singlet energy for  $A \rightarrow A^*$ . The solution Fermi level (electrochemical potential) is established by the  $A^+/A$  couple and is more positive than  $E^{\circ}(A^+, A)$ , since  $[A^+] > [A]$ . Schematically, an electron is injected from the metal into the lowest unoccupied orbital of  $A^+$  rather than into the singly occupied lower orbital. This direct excitation process would not occur at a film-free metal electrode, since electron injection into the lower orbital from available electronic levels in the metal is always favored. For this experiment to be unambiguous, no reduced form of  $A$  (i.e.,  $A^-$ ) should be formed at  $E_{\text{c}}$  to avoid the possibility of annihilation ECL between  $A^-$  and  $A^+$  producing  $A^*$ .

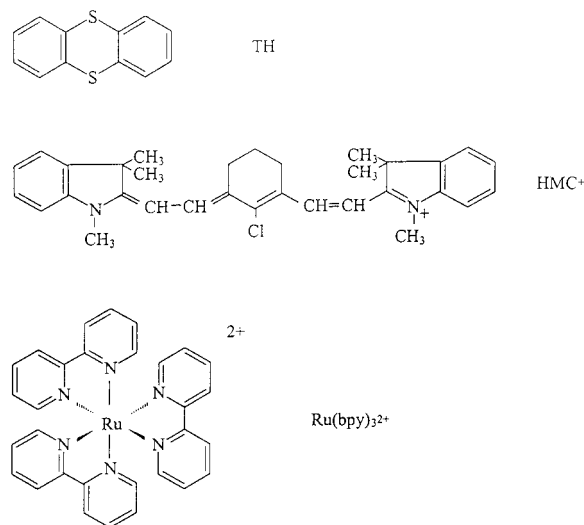


Neither should the solution contain a coreactant like  $\text{S}_2\text{O}_8^{2-}$  that can generate a strong oxidant (e.g.,  $\text{SO}_4^{\bullet-}$ ) upon reduction, since this can also produce solution-phase ECL via the reaction<sup>12</sup>



Finally, the oxide film should be stable during the cathodic pulsing. The molecules selected in this study were the oxidized forms of thianthrene (TH), the heptamethine cyanine dye,  $\text{HMC}^+$ , and  $\text{Ru}(\text{bpy})_3^{2+}$ . Only with the latter compound is annihilation ECL possible.

Related studies of this type have been reported by Kulmala and co-workers,<sup>13</sup> e.g., using an oxide-covered Al electrode in aqueous media. However, in many cases in these studies the solution contained the coreactant  $\text{S}_2\text{O}_8^{2-}$  so that annihilation ECL between a reduced species produced at the electrode and  $\text{SO}_4^{\bullet-}$  could not be ruled out.<sup>12</sup> Moreover, the  $\text{Al}_2\text{O}_3$  film is not very stable during cathodization in aqueous solution, probably because the buildup of basicity during hydrogen evolution promotes film dissolution. We have selected  $\text{Ta}_2\text{O}_5$  in this study because it is a large band-gap material that is chemically and electrochemically stable and its film formation,



e.g., by anodization, has been widely studied. Moreover, we have selected an aprotic solvent, MeCN, to avoid possible complications with hydrogen evolution at the cathode or oxygen production (with possible intermediates) at the counter electrode. Other studies have also reported formation of excited states by direct heterogeneous electron transfer at semiconductor electrodes such as n-ZnO and n-CdS,<sup>14–16</sup> although the process was not described in terms of hot electrons. We also report here the comparative electrochemical behavior of a number of nernstian one-electron redox couples at Pt and  $\text{Ta}_2\text{O}_5$  to assist in locating the  $\text{Ta}_2\text{O}_5$  energy levels and gap states.

## Experimental Section

The supporting electrolyte used in all experiments was polarographic grade tetra-*n*-butylammonium perchlorate (TBAP, SACHEM, Austin, TX), and it was dried and purified as described previously.<sup>17</sup> UV grade (0.0001% water) acetonitrile (MeCN, Burdick and Jackson) was used as received after being transported unopened into an inert atmosphere drybox (Vacuum Atmospheres). Tris(2,2'-bipyridyl)ruthenium(II) perchlorate ( $\text{Ru}(\text{bpy})_3(\text{ClO}_4)_2$ ) was prepared by metathesis of  $\text{Ru}(\text{bpy})_3\text{Cl}_2 \cdot 6\text{H}_2\text{O}$  (Aldrich) with an excess of  $\text{NaClO}_4$  in  $\text{H}_2\text{O}$ . The crystals were washed with  $\text{H}_2\text{O}$ , recrystallized from EtOH and MeCN, and dried under vacuum at 90 °C for 24 h. Thianthrene (Aldrich) was recrystallized 3 times from xylene/MeOH under nitrogen in subdued light and dried under vacuum at 80 °C. Heptamethine cyanine (IR 789, Aldrich) was used without further purification. In the electrochemistry experiments at Pt and Ta, most of the compounds were obtained from commercial sources and in most cases were purified by two or three recrystallizations from the appropriate solvent. The concentration of solute for each solution was generally 2 mM. All samples, solvents, and electrolytes were prepared in a drybox under a He atmosphere and were sealed in airtight vessels for measurements made outside the drybox.

Different forms of tantalum (wire, plate, rod, foil; Aldrich, 99.999%) were used as electrodes. In most cases, native oxide films, about 2.5 nm thick, formed in air were present on the surface. The electrodes for ECL had geometric areas of 0.3–0.5 cm<sup>2</sup>. Thicker oxide films were produced both thermally and anodically, and the effect of oxide film thickness on ECL was studied. Before anodization, the electrodes were polished mechanically with 0.05  $\mu\text{m}$  alumina and then cleaned ultrasonically. Anodization was usually performed in a 0.1 M ammonium tartrate (Matheson, Coleman & Bell) solution (pH =

6.7). In the electrochemical studies the Pt working electrode was a flat disk (about 0.03 cm<sup>2</sup>) sealed in glass. A piece of Ta, cut from a rod and sealed in glass with silicone cement to yield a disk with an area of about 0.03 cm<sup>2</sup>, was used as the Ta/Ta<sub>2</sub>O<sub>5</sub> working electrode. Before each experiment, these electrodes were polished with 1 and 0.3 μm alumina powder. The reference electrode was a silver wire that was introduced in a separate chamber closed with a fritted glass disk to avoid any contamination during the experiments. The auxiliary electrode was platinum mesh (area = 2 cm<sup>2</sup>).

X-ray photoelectron spectroscopy (PHI 5700 ESCA system, Physical Electronics) was used to determine the oxide thickness and surface cleanliness and composition. An AlKα (1487.7 eV) anode and a hemispherical electron energy analyzer were used. The experiments were carried out in an ultrahigh vacuum system (base pressure = 10<sup>-10</sup> Torr).

The electrochemical ECL cell was of a conventional design. Bulk electrolysis experiments were performed using a Princeton Applied Research (PAR) model 173/175 potentiostat/universal programmer. The working electrode was a large Pt mesh (surface area ≈ 4 cm<sup>2</sup>), and a Pt mesh counter electrode was located in a compartment separated from the bulk solution by a fine frit. For standard cyclic voltammetric (CV) measurements, a silver wire was used as a quasireference electrode (AgQRE) and its potential was calibrated versus ferrocene (i.e., the Fc/Fc<sup>+</sup> couple) by adding SCE and recording its CV wave at Pt. All potentials are reported vs aq SCE by taking  $E_{1/2}(\text{Fc}/\text{Fc}^+) = +0.307 \text{ V vs aq SCE}$ .<sup>18</sup> Controlled potential ECL and CV experiments were carried out with a PAR model 175 programmer and model 173/176 potentiostat and a CH Instruments (Memphis, TN) model 660 electrochemical work station. ECL measurements were performed as previously reported<sup>19</sup> using a charge-coupled device (CCD) camera (model CH260, Photometrics, Tucson, AZ) cooled to -130 °C. The spectrometer was calibrated with a Hg-Ar test lamp (Ultra-Violet Products, San Gabriel, CA). Experiments were performed in the darkroom, and care was taken to eliminate stray light.

A Xe lamp (Christie Electric Corp., Los Angeles, CA) operated at 2500 W was used as the light source for the photocurrent measurements. A quartz cell was used for measurements in the UV region. A water filter was used to remove infrared radiation in the measurement of the conduction band edge (flat band potential). The band gap of the Ta electrode was taken as 4.0 eV.<sup>20</sup>

## Results

To describe the energetics of the Ta/Ta<sub>2</sub>O<sub>5</sub>/MeCN system, it is necessary to establish the locations of the band edges in the oxide with respect to solution redox levels. This approach is also useful in locating surface state energies.

**Estimation of Conduction Band Edge Energy from Photocurrent Measurements.** The current-potential curves for Ta/Ta<sub>2</sub>O<sub>5</sub> in 0.1 M TBAP/MeCN under illumination by a Xe lamp and in the dark are shown in Figure 2. Upon irradiation of the electrode through the electrolyte, an anodic photocurrent appears. The Fermi level of the oxide is determined from the flatband potential, which can be estimated from the potential for the onset of the photocurrent because photocurrent requires band bending in the oxide to move photogenerated holes to the interface. Generally, the potential for photocurrent onset is somewhat positive of the actual flatband potential because of photogenerated carrier recombination at small band bending. We find the photocurrent onset at -1.1 V vs SCE (Figure 2). Electrochemically generated Ta oxides are usually of a heavily

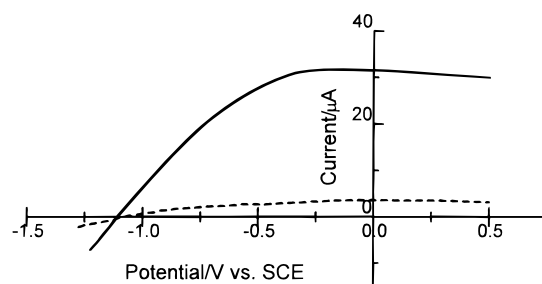


**Figure 2.** Current-potential curves for a Ta/Ta<sub>2</sub>O<sub>5</sub> electrode in 0.1 M TBAP/MeCN (—) under illumination with a 2500 W Xe lamp and (---) without illumination; scan rate = 100 mV/s.

**TABLE 1: Potential (in V vs Fc<sup>+</sup>/Fc) at Pt and Ta/Ta<sub>2</sub>O<sub>5</sub> Electrodes<sup>a</sup>**

compd	potential vs Fc (V)			$E_{pc}$ at Ta/Ta <sub>2</sub> O <sub>5</sub> <sup>c</sup>
	$E_{1/2}$ at Pt <sup>b</sup>			
	first wave	second wave	third wave	
TCNQ	0	-0.6		-1.5
<i>p</i> -chloranil	-0.4	-1.2		-1.6
MV <sup>2+</sup> (MVPF <sub>6</sub> )	-0.8	-1.2		-1.6
duroquinone	-1.2	-2.0		-2.2
S <sub>2</sub> O <sub>8</sub> <sup>2-</sup>	-1.4 <sup>b</sup>			-2.4
((TBA) <sub>2</sub> S <sub>2</sub> O <sub>8</sub> )				
9-fluorenone	-1.7	-2.7		-2.2
Ru(bpy) <sub>3</sub> <sup>2+</sup>	-1.7	-1.9	-2.1	-2.1
phthalonitrile	-2.1			-2.6
pyrene	-2.5			-2.8
naphthalene	-3.0			

<sup>a</sup> Potential (V vs SCE) = potential (V vs Fc<sup>+</sup>/Fc) + 0.3. <sup>b</sup>  $E_{1/2}$  estimated as average of cathodic and anodic peak potentials ( $E_{pc}$  and  $E_{pa}$ ). <sup>c</sup> Cathodic peak potential.

doped n-type.<sup>20</sup> Thus, the Fermi level lies relatively close, i.e., within a few tenths of an electronvolt, to the bottom of the conduction band,  $E_c$ , so determination of the Fermi-level energy provides an estimate of  $E_c$ . This curve in MeCN is similar to that found in water.<sup>21</sup>

**Electrochemical Measurements at Pt and Ta.** One approach to location of the conduction band and mapping the band-gap region for states that allow electron transfer to solution species is to carry out comparative CV experiments for one-electron species at both Pt and the electrode of interest. This approach has previously been used for TiO<sub>2</sub> in acetonitrile.<sup>22</sup> The list of the compounds used in the electrochemical study are given in Table 1. These species were chosen because the potentials for their first reductions were at sufficiently negative values to be in the vicinity of the conduction-band energies of Ta<sub>2</sub>O<sub>5</sub>, allowing evaluation where significant faradaic currents were observed.

In all cases, the first reduction waves on Pt were characteristic of nernstian waves, except for S<sub>2</sub>O<sub>8</sub><sup>2-</sup>. Figure 3 shows the CVs for methyl viologen (MV<sup>2+</sup>), duroquinone, and fluorenone in MeCN at Pt and at Ta<sub>2</sub>O<sub>5</sub> at a scan rate,  $v$ , of 0.1 V/s. The CV of MV<sup>2+</sup> at Pt consists of two cathodic waves at -0.5 and -0.9 V vs SCE, while the CV recorded with the same solution at Ta/Ta<sub>2</sub>O<sub>5</sub> shows that the redox potential of MV<sup>2+</sup> is shifted to a more negative potential, with the current increasing significantly only at -1.3 V vs SCE. The CV on Ta/Ta<sub>2</sub>O<sub>5</sub> consists of two reduction waves with a shoulder that can probably be assigned to the reduction of MV<sup>2+</sup>.

The same experiments were carried out with 10 other couples, and the results are summarized in Figure 4. For all the experiments, a small residual current was generally observed

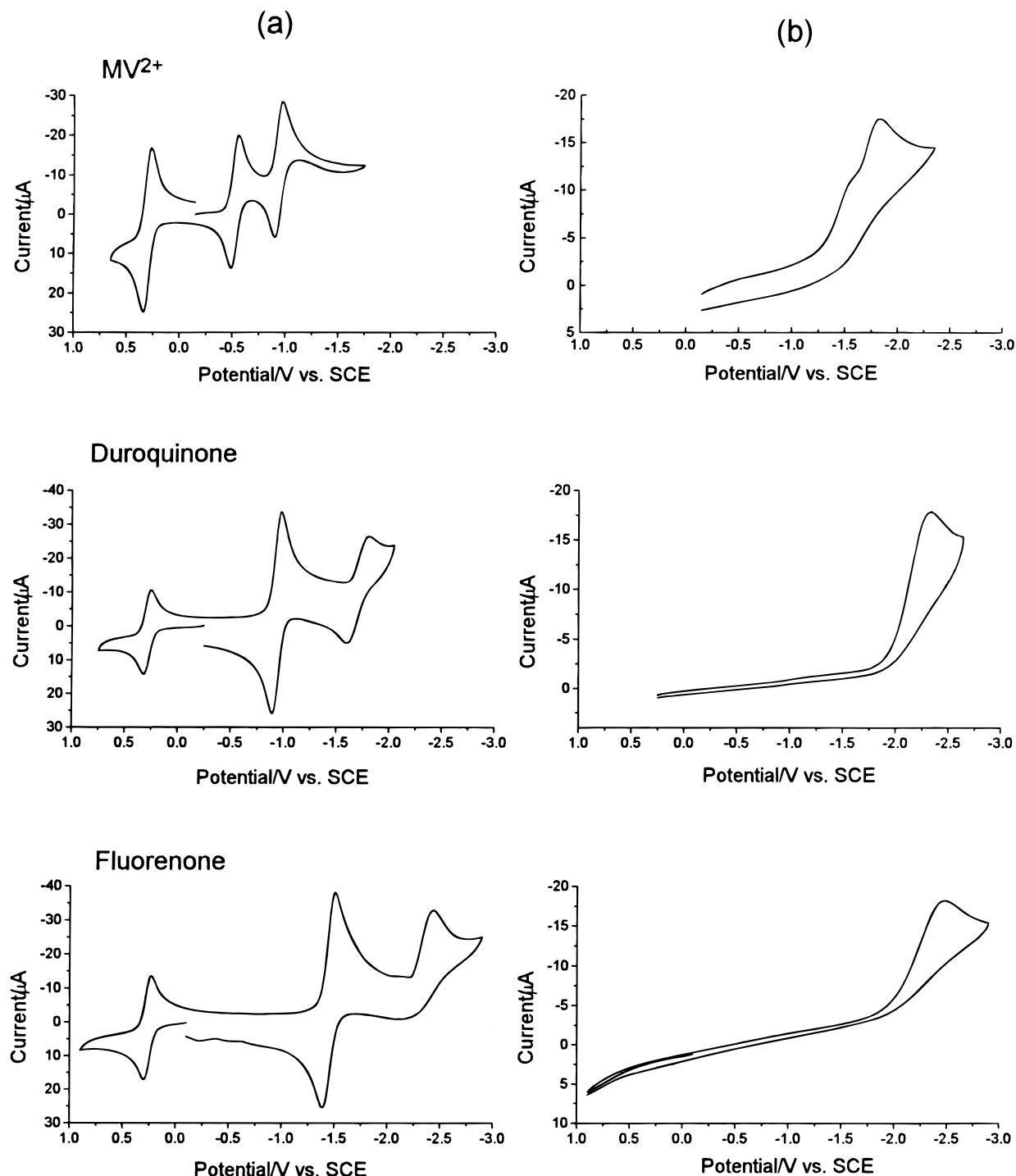


**Figure 3.** Cyclic voltammograms for the reduction of 2 mM  $MV^{2+}$ , duroquinone, and fluorenone in MeCN/0.1 M TBA(PF)<sub>6</sub> at (a) Pt and (b) Ta/Ta<sub>2</sub>O<sub>5</sub> electrodes; scan rate = 0.1 V/s.

on Ta/Ta<sub>2</sub>O<sub>5</sub> before the reduction of the species, which increased linearly with potential. The main observation shows that for all of the couples the potentials for the reductions were shifted to more negative values at Ta<sub>2</sub>O<sub>5</sub> and no reduction occurred at a potential more positive than -1.2 V vs SCE (Figure 4). As shown in this figure, for those compounds with redox potentials at Pt between 0 and -1 V (e.g., TCNQ, p-chloranil,  $MV^{2+}$ ), their reduction potentials were shifted to a value more negative than -1.2 V at Ta<sub>2</sub>O<sub>5</sub>. For the other couples (e.g., Ru(bpy)<sub>3</sub><sup>2+</sup>, fluorenone), their potentials at Ta<sub>2</sub>O<sub>5</sub> were shifted to a value more negative than -1.7 V. In all cases, chemical reversibility

of the waves on Ta<sub>2</sub>O<sub>5</sub> was never observed and the current, normalized to unit area, was larger on Pt than on the Ta/Ta<sub>2</sub>O<sub>5</sub> electrode.

**Electrogenerated Chemiluminescence. Thianthrene.** Thianthrene (TH) is oxidized at a Pt electrode to a stable radical cation at  $E_{pa} = 1.2$  V vs SCE (Figure 5a). TH is not reducible in MeCN/TBAP at Pt at potentials up to the solvent background, -2.4 V vs SCE. A solution containing the oxidized precursor (TH<sup>•+</sup>) was prepared by bulk electrolysis at a large Pt electrode at 1.4 V vs SCE. CVs taken before and after addition of 7 mM TH<sup>•+</sup> in 0.1 M TBAP/MeCN at a Ta electrode are shown

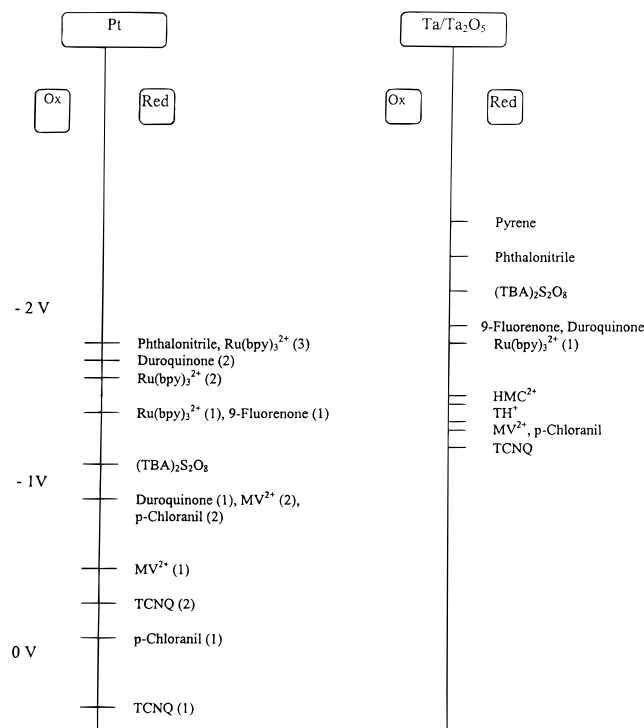


**Figure 4.** Redox potentials in V vs SCE of the compounds studied at the Pt and Ta/Ta<sub>2</sub>O<sub>5</sub> electrodes. Potentials were obtained at a scan rate of 0.1 V/s (see Table 1 for potentials vs Fc<sup>+</sup>/Fc).

in Figure 5b. When TH<sup>+</sup> was added, only a very small increase of current was seen below -1.5 V.

Pulsing to potentials more negative than -2 V vs SCE produced higher currents and light emission. Plots of the ECL spectra as a function of potential are shown in Figure 5c. The potential of the Ta/Ta<sub>2</sub>O<sub>5</sub> electrode was pulsed between 0 V and the negative potentials shown with 0.1 s step widths. ECL was produced at potentials more negative than about -2 V vs SCE, and the ECL intensity increased with potential between -2 and -3 V. The ECL spectra showed a maximum at about 500 nm, identical with the previous literature ECL spectrum of TH,<sup>23</sup> so the emitting species can be identified as the first excited singlet state of TH. However, at potentials above -3.0 V (Figure 5), a new ECL signal appeared at 650–700 nm. This kind of emission has previously been seen in MeCN containing only TBABF<sub>4</sub> (tetra-*n*-butylammonium tetrafluoroborate) as a supporting electrolyte at very negative potentials (< -3.5 V vs Ag) at a Pt electrode and was attributed to the formation of oligomers or polymers of MeCN.<sup>24</sup> Moreover, electroluminescence of Ta<sub>2</sub>O<sub>5</sub> is possible at very negative potentials.<sup>25</sup>

To demonstrate direct excited-state production via heterogeneous electron transfer at the electrode, and not emission from a homogeneous radical ion annihilation or an impurity coreactant pathway, the same experiments were carried out with Pt and Au electrodes under identical conditions. No ECL was detected at a Pt or Au electrode in a TH<sup>+</sup> solution when the potential was pulsed between 0 V and -1 to -2.5 V, eliminating a homogeneous electron-transfer path leading to excited states. Thus, the emission observed at Ta can be attributed to the following mechanism.

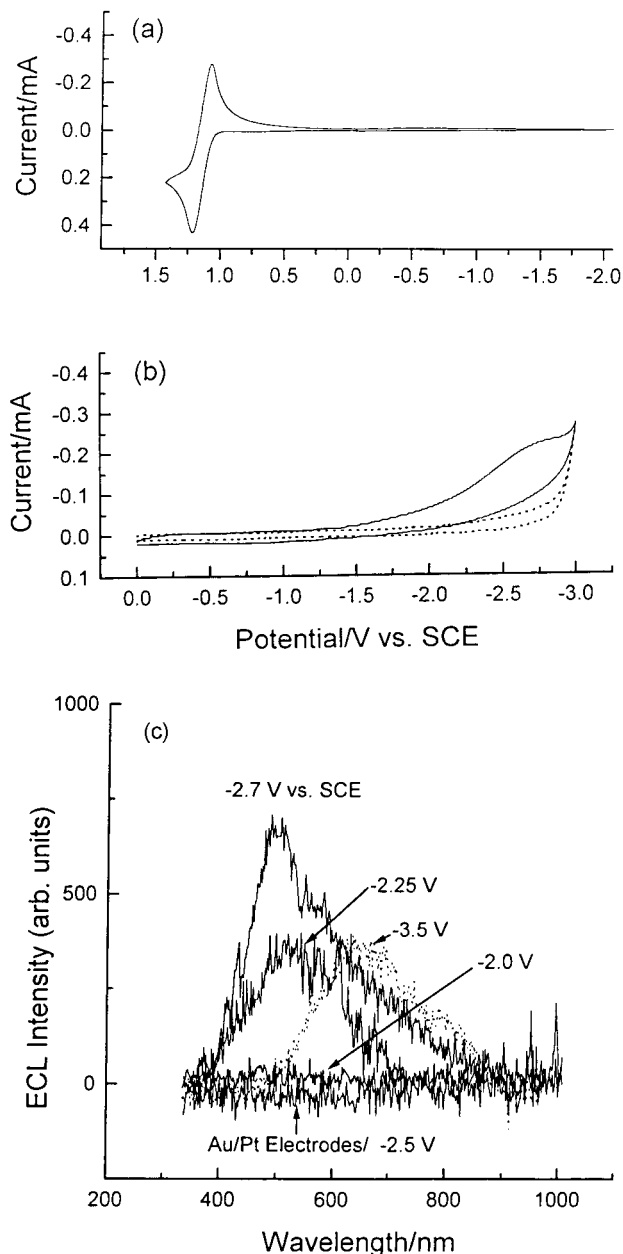


**Figure 5.** Cyclic voltammograms and ECL spectra of 7 mM TH solutions in MeCN/0.1 M TBAP: (A) TH at a Pt electrode, scan rate = 0.1 V/s; (B) TH<sup>+</sup> at a Ta/Ta<sub>2</sub>O<sub>5</sub> electrode, scan rate = 1 V/s, dashed curve represents data in absence of TH<sup>+</sup>; (C) ECL of TH<sup>+</sup> as a function of the cathodic pulse potential of the Ta/Ta<sub>2</sub>O<sub>5</sub> electrode. Potential was pulsed between 0 V and the potentials indicated at a cycling frequency of 10 Hz; total exposure time = 5 min.

*Heptamethine cyanine Dye (HMC<sup>2+</sup>)*. The same type of experiment was carried out with the HMC dye.<sup>19</sup> HMC<sup>+</sup> at a Pt electrode is reversibly oxidized in a one-electron transfer step at  $E_{\text{pa}} = 0.50$  V vs SCE (Figure 6a). A solution of HMC<sup>2+</sup> was prepared by bulk electrolysis at 0.7 V vs SCE. Figure 6b shows the CV of a Ta electrode in MeCN/0.1 M TBAP with and without 5 mM HMC<sup>2+</sup>. The current scan showed a small current increase around -2 V when HMC<sup>2+</sup> was added in TBAP electrolyte solution. The ECL spectra obtained during cathodic pulsing at Ta/Ta<sub>2</sub>O<sub>5</sub> are shown in Figure 6c. ECL was observed only when the potential was more negative than -2 V. The ECL spectra exhibited a maximum intensity at about 800 nm, identical with the previous ECL spectrum obtained by

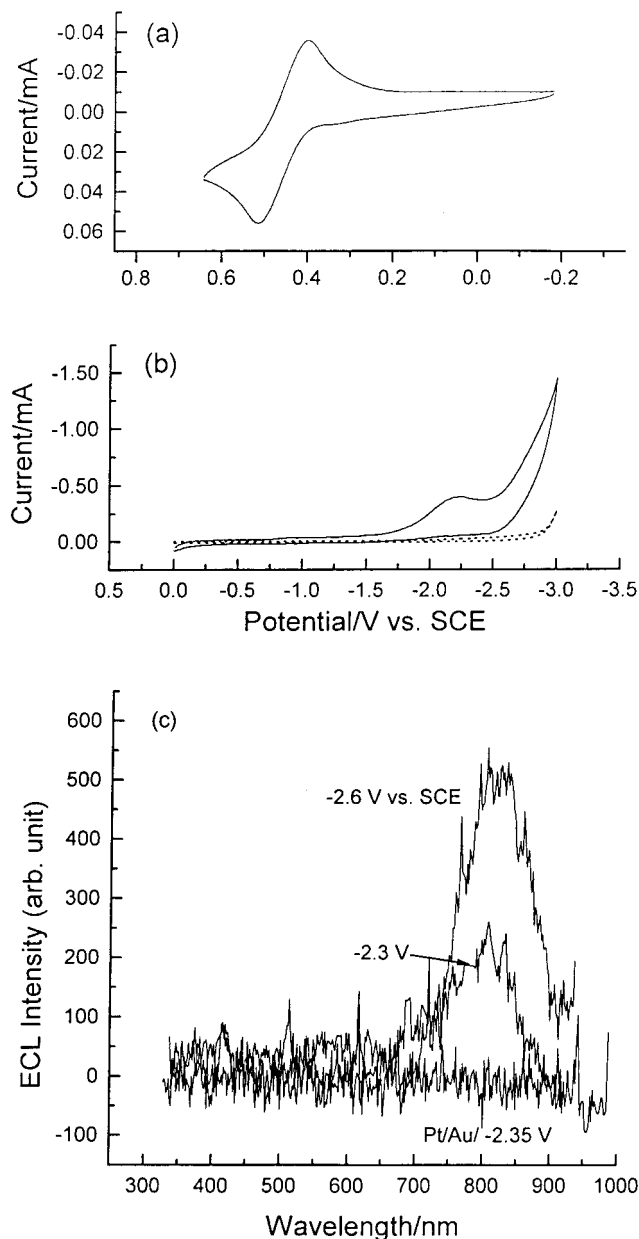
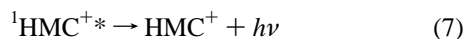


**Figure 6.** Cyclic voltammograms and ECL spectra of HMC solutions in MeCN/0.1 M TBAP: (A) 1 mM HMC<sup>+</sup> at a Pt electrode, scan rate = 1 V/s; (B) 1 mM HMC<sup>2+</sup> at a Ta/Ta<sub>2</sub>O<sub>5</sub> electrode, scan rate = 1 V/s, dashed curve represents data in absence of HMC<sup>2+</sup>; (C) ECL of HMC<sup>2+</sup> (0.25 mM) as a function of the cathodic pulse potential of the Ta/Ta<sub>2</sub>O<sub>5</sub> electrode. Potential was pulsed between 0 V and the potentials indicated at a cycling frequency of 10 Hz; total exposure time = 20 min.

oxidation of HMC<sup>+</sup> in the presence of a coreactant.<sup>19</sup> Again, no emission was detected at the Pt and Au electrodes in the HMC<sup>2+</sup> solution when the potential was pulsed between 0 V and -1 to -2.5 V, so ECL does not occur at these electrodes under conditions where ECL is observed at the Ta electrode. Thus, we again propose a hot-electron mechanism.



*Ru(bpy)<sub>3</sub><sup>3+</sup>*. *Ru(bpy)<sub>3</sub><sup>2+</sup>* oxidizes at a Pt electrode to a stable cation radical with  $E_{pa} = 1.25$  V vs SCE (Figure 7a). A solution

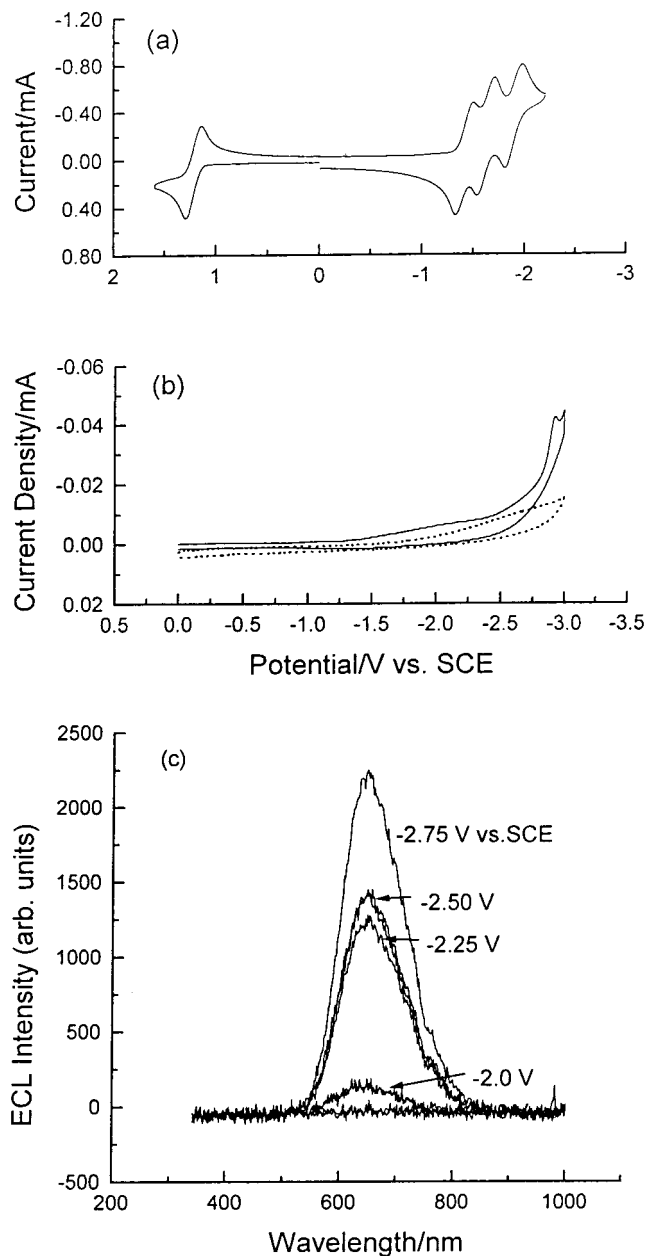


**Figure 7.** Cyclic voltammograms and ECL spectra of *Ru(bpy)<sub>3</sub><sup>2+</sup>* solutions in MeCN/0.1 M TBAP; (A) 1 mM *Ru(bpy)<sub>3</sub><sup>2+</sup>* at a Pt electrode, scan rate = 0.1 V/s; (B) 0.5 mM *Ru(bpy)<sub>3</sub><sup>3+</sup>* at a Ta/Ta<sub>2</sub>O<sub>5</sub> electrode, scan rate = 1 V/s, dashed curve represents data in absence of *Ru(bpy)<sub>3</sub><sup>3+</sup>*; (C) ECL of *Ru(bpy)<sub>3</sub><sup>3+</sup>* (0.5 mM) as a function of the cathodic pulse potential of the Ta/Ta<sub>2</sub>O<sub>5</sub> electrode. Potential was pulsed between 0 V and the potentials indicated at a cycling frequency of 10 Hz; total exposure time = 30 s.

containing the *Ru(bpy)<sub>3</sub><sup>3+</sup>* precursor was prepared by bulk electrolysis at 1.5 V vs SCE. CVs taken before and after the addition of 1 mM *Ru(bpy)<sub>3</sub><sup>3+</sup>* in 0.1 M TBAP/MeCN at a Ta electrode are shown in Figure 7b. When *Ru(bpy)<sub>3</sub><sup>3+</sup>* was added, the current increased at potentials more negative than -1.5 V.

Pt, Au, and Ta electrodes of similar size were used with *Ru(bpy)<sub>3</sub><sup>3+</sup>* to compare the ECL intensity. Figure 7c shows the ECL spectra at a Ta electrode. Unlike the behavior found with TH and HMC, Pt and Au electrodes showed ECL signals (Figure 8) at potentials below -1.2 V. *Ru(bpy)<sub>3</sub><sup>3+</sup>* can produce ECL via an annihilation mechanism by reaction with electrogenerated *Ru(bpy)<sub>3</sub><sup>3+</sup>*.<sup>26</sup> The results in Figure 8 suggest this route because

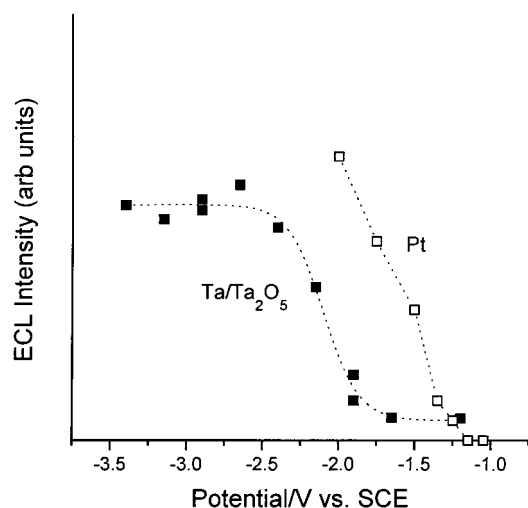
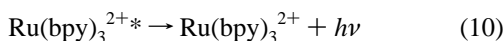
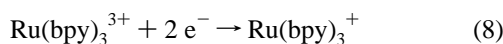


**Figure 8.** ECL intensity of  $\text{Ru}(\text{bpy})_3^{3+}$  (0.5 mM) as a function of the cathodic pulse potential of Pt and Ta/Ta<sub>2</sub>O<sub>5</sub> electrodes. Potential was pulsed between 0 V and the potentials indicated at a cycling frequency of 10 Hz.

$\text{Ru}(\text{bpy})_3^{3+}$  formation starts at  $-1.1$  V at Pt (Figure 7a). The annihilation reaction scheme is as follows:



ECL was observed at Ta only when the potential was more negative than  $-2$  V. In this potential region, at least a part of the ECL originates from reduction of  $\text{Ru}(\text{bpy})_3^{3+}$  to  $\text{Ru}(\text{bpy})_3^+$ , as observed at Pt electrodes. It is possible, however, that a portion of the luminescence occurs via hot electron transfer from the electrode directly to the  $\text{Ru}(\text{bpy})_3^{3+}$  to produce the excited state.

**ECL Efficiency.** The ECL emission intensity is low. Apparatus and methodologies for the measurement of ECL efficiencies have been reported previously.<sup>23,27</sup> ECL efficiency or yield,  $\phi_{\text{ECL}}$ , is defined here as photons emitted per electron passed.<sup>27</sup> The  $\phi_{\text{ECL}}$  for the hot-electron mechanism was determined by comparing the photons of light produced per coulomb passed with a standard whose ECL efficiency is known. Using  $\text{Ru}(\text{bpy})_3^{2+}$  as a standard,<sup>28</sup> we obtained ECL efficiencies of  $0.002 \pm 0.0015$  for  $\text{TH}^{+}$  and  $0.003 \pm 0.0015$  for  $\text{HMC}^{2+}$ . That is, for each 1000 molecules formed by reduction at the Ta working electrode, approximately 2–3 photons are produced by hot electrons.

The fluorescence efficiency for TH is about 0.04; thus, in the absence of additional quenching of  $\text{TH}^*$  at the electrode surface, the relative efficiency for excited-state production via hot solution electrons is about 0.05. The low efficiency can be ascribed to rapid relaxation of the hot electrons, e.g., at the oxide surface through surface states, so that most of the current leads to formation of ground-state species (TH or  $\text{HMC}^+$ ).

#### Effect of Oxide Film Thickness and Surface Modification.

The flow of electrons through oxide films has been discussed extensively.<sup>29–31</sup> At the thickness of interest here,  $\geq 2.5$  nm, direct tunneling from the metal to solution species probably does not make a major contribution. Rather, electrons are probably injected into the Ta<sub>2</sub>O<sub>5</sub> conduction band and transported to the solution interface. Possible modes for conduction-band transport are discussed in the next section. To study these effects, we

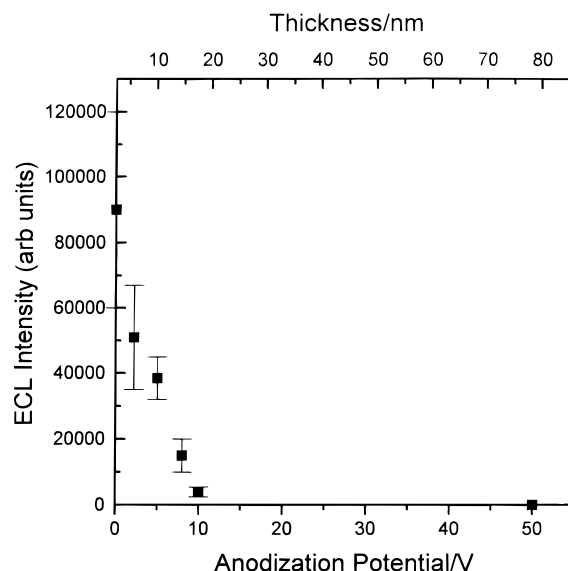


**Figure 9.** ECL intensity for  $\text{TH}^+$  reduction as a function of Ta<sub>2</sub>O<sub>5</sub> thickness. Ta<sub>2</sub>O<sub>5</sub> formed anodically at room temperature in 0.1 M ammonium tartrate. ECL was generated with a 0 to  $-3$  V pulse (10 Hz frequency) in MeCN/0.1 M TBAP, and the signal was integrated for 5 min.

performed the same ECL experiments as discussed above with different thicknesses of oxide (Figure 9). The oxide film was formed anodically in 0.1 M ammonium tartrate, pH 6.7, at different applied voltages; for Ta<sub>2</sub>O<sub>5</sub>, the corresponding proportionality factor is  $16.7 \text{ \AA/V}$ .<sup>32</sup> The ECL signal, in all cases obtained by pulsing between 0 and  $-3$  V at 10 Hz in MeCN/0.1 M TBAP, showed a linear decrease with increasing oxide thickness, with essentially no emission observed for films prepared at voltages above 10 V, corresponding to a film thickness of 20 nm. The potential for the onset of current,  $-1.6 \pm 0.1$  V vs SCE, was independent of oxide thickness, suggesting that electron injection via the conduction band of Ta<sub>2</sub>O<sub>5</sub> predominated.

Etching or cleaning the oxide-filmed Ta electrode in HF or 1:1:1 HF/HNO<sub>3</sub>/H<sub>2</sub>O or 9:1 NaOH/H<sub>2</sub>O did not lead to an increase in light intensity. We also attempted surface modification by silanization<sup>33</sup> of the Ta<sub>2</sub>O<sub>5</sub> surface in an attempt to block or passivate surface states that may be involved with thermalization of the hot electrons. The Ta/Ta<sub>2</sub>O<sub>5</sub> electrode was treated in a glovebox with a 1% solution of 3-(2-aminoethylamino)-propyltrimethoxysilane in benzene at room temperature for 24 h followed by rinsing 3 times with benzene and MeCN. XPS analysis of the electrode following this treatment showed peaks for Si, N, and C, indicating that silanization occurred. However, the ECL signal was almost totally absent on the silanized electrode, suggesting that this treatment formed a film on the electrode surface that hindered electron transfer to the solution species or blocked active sites needed for the electron transfer. Experiments on surface modification with a Pt film on the Ta<sub>2</sub>O<sub>5</sub> surface are discussed in the following paper.<sup>34</sup>

#### Discussion

The energy levels (taken as potentials vs aq SCE) in the Ta/Ta<sub>2</sub>O<sub>5</sub>/MeCN solution system based on the described measurements are shown in Figure 10. The electronic states of the Ta<sub>2</sub>O<sub>5</sub> film mainly consist of oxygen anion states forming the valence band and metal cation (Ta 5d states) forming the conduction band with a band gap of 4.0 eV.<sup>20</sup> Impurity atoms and defect states (e.g., oxygen vacancies) result in doping and

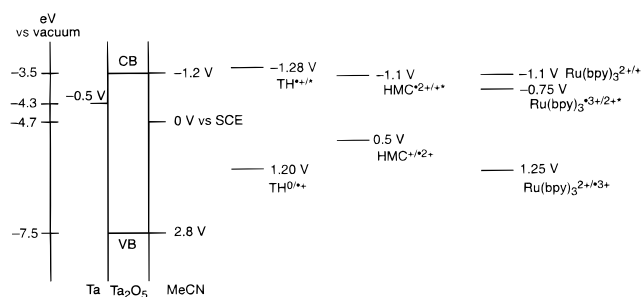
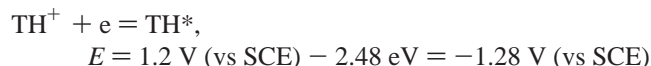


**Figure 10.** Proposed approximate energy levels for Ta/Ta<sub>2</sub>O<sub>5</sub>/MeCN system. All potentials shown are in V vs aq SCE. CB and VB mark the conduction and valence bands from photocurrent measurements. For reference,  $E(\text{Fc}^+/\text{Fc})$  in MeCN = 0.307 V vs aq SCE.

localized states within the band gap.<sup>35</sup> The film is n-type and usually contains a high concentration ( $10^{17}$ – $10^{20}$  cm<sup>-3</sup>) of oxygen vacancies. From these considerations, the open circuit Fermi level probably lies 0.1–0.4 eV below the conduction band. Thus, taking the photocurrent onset as the flatband potential, -1.1 V vs SCE (Figure 2), and considering possible recombination effects in the measurement and doping levels, we place the conduction band edge at -1.2 to -1.5 V vs SCE. This level is consistent with the measurements of the various redox couples in Figure 4.

The work function of Ta was taken as 4.25 eV, placing the Ta Fermi level at about -0.5 V vs aq SCE (taking the location of the standard hydrogen electrode as -4.5 eV). This would suggest a Schottky barrier at the Ta/Ta<sub>2</sub>O<sub>5</sub> interface of about 0.7 eV. The solution-phase energy levels for ground-state species, e.g., TH/TH<sup>+</sup>, are based on the cyclic voltammetric measurements. In all cases where ECL occurs, these levels serve to establish the Fermi level in solution. Since in these experiments the oxidized form, produced in a controlled potential electrolysis, was in excess, the actual Fermi levels are at somewhat more positive potentials than the  $E_{1/2}$  values indicated in Figure 10. The energy levels for production of the excited states (V vs SCE) were obtained from the energy for the ground-state process ( $\text{A}^+ + \text{e} = \text{A}$ ) and the excitation energy to form the appropriate excited state. For TH, we obtain



Thus, an electron with an energy at the Ta<sub>2</sub>O<sub>5</sub> conduction band edge would be sufficient, within the uncertainties in energies, to form TH\*. The energy level for the reaction of HMC<sup>2+</sup> to form HMC<sup>•+</sup> is 0.5 V - 1.6 eV (800 nm) = -1.1 V vs SCE, again consistent with a conduction band edge electron emitted into the solution. The situation for Ru(bpy)<sub>3</sub><sup>2+</sup> is more complicated since two energy levels are accessible to conduction band electrons Ru(bpy)<sub>3</sub><sup>3+</sup>/Ru(bpy)<sub>3</sub><sup>2+•</sup> and Ru(bpy)<sub>3</sub><sup>3+</sup>/Ru(bpy)<sub>3</sub><sup>•+</sup>. Hot electrons in the solution would be involved in both reduction processes. The fact that the emission from the Ru(bpy)<sub>3</sub><sup>2+</sup> system is higher than that for the others suggests an appreciable contribution from the annihilation route.

We now consider electron transport from Ta to the solution species. Transport through oxide films has been discussed extensively,<sup>29,30–31</sup> including the particular case of Ta<sub>2</sub>O<sub>5</sub> in Ta/Ta<sub>2</sub>O<sub>5</sub>/M (M = Au, Pt, Al) structures.<sup>35</sup> A schematic diagram of the system considered here is shown in Figure 11. Tunneling of electrons through the oxide film to solution species by “direct tunneling”<sup>31a</sup> would probably follow an exponential dependence on thickness,  $x$ , and  $\phi^{1/2}$ , where  $\phi$  is the potential drop across

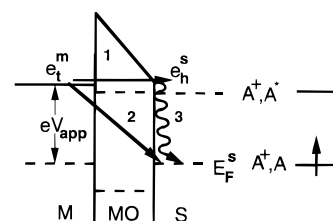


**Figure 11.** Schematic diagram for electron transfer from Ta to solution: (path 1) through Ta<sub>2</sub>O<sub>5</sub> conduction band; (path 2) relaxation in bulk semiconductor (e.g., via traps); (path 3) relaxation via surface states on Ta<sub>2</sub>O<sub>5</sub> or in solution.

the film, as is found in scanning tunneling microscopy,

$$i \propto \exp(-\beta x \phi^{1/2})$$

where  $\beta \approx 1 \text{ \AA}^{-1}$ .<sup>36</sup> Even with the thickness of native oxide being 2.5–3 nm, direct tunneling should not be an important path in electron transfer. Indeed, the electrochemical measurements summarized in Figure 4 support this assertion. For example, the currents at Ta/Ta<sub>2</sub>O<sub>5</sub> for TCNQ and TH<sup>+</sup>, with quite positive redox potentials, do not start until potentials near the conduction band edge, even though the driving force for electron transfer, which is related to  $\phi$ , is large. This is also consistent with the fact that all electron transfers occur near -1.5 V vs SCE. It is more likely that electrons are injected into the conduction band of Ta<sub>2</sub>O<sub>5</sub> from the Ta when they move to the Ta<sub>2</sub>O<sub>5</sub>/MeCN interface (indicated as path 1). The question of injection across the barrier at the Ta/Ta<sub>2</sub>O<sub>5</sub> interface is common to many oxide films, and the lack of rectification is often attributed to the presence of defects or impurity states at the interface that provide paths for electron transfer.<sup>29</sup> Mead's experiments<sup>35</sup> suggest that electron transport through Ta<sub>2</sub>O<sub>5</sub> films is limited by the bulk material and not interfacial potential barriers. He estimates that the mean free path of electrons in Ta<sub>2</sub>O<sub>5</sub> is probably less than 10 Å so that injected electrons largely thermalize in the Ta<sub>2</sub>O<sub>5</sub> and arrive at the interface with MeCN at an energy characteristic of the conduction band edge. Note that even at this energy, given uncertainties in the energetic location, electrons are sufficiently energetic to form the excited states of TH, HMC<sup>+</sup>, and Ru(bpy)<sub>3</sub><sup>2+</sup>. Population of the ground states directly (indicated by path 2), e.g., via traps or levels in the gap or phonon emission, is unlikely to be significant, so the observed low efficiency of ECL must be attributed to the thermalization of hot electrons in solution or on the Ta<sub>2</sub>O<sub>5</sub> surface, e.g., via surface state levels, or by quenching of the excited states. However, quenching of the excited states via energy or electron transfer to the Ta should be no larger than that found in ECL at Pt electrodes. Annihilation ECL of TH and HMC<sup>+</sup> produces much higher intensities at Pt than seen here, although in those cases excited-state formation occurs farther from the electrode surface. Other studies of immobilized species on electrodes produce appreciable ECL emission,<sup>37</sup> so metal quenching of the excited state is probably not the major source of inefficiency. Rather thermalization of hot electrons via surface processes (path 3) probably is the main cause of inefficiency. Although surface modification by silanization does not improve the ECL yield, we show in the following paper that a Pt film on the Ta<sub>2</sub>O<sub>5</sub> surface produces significant increases.

In describing a reaction as a “hot-electron” process in the solution phase,<sup>10,11,13</sup> we mean that the hot electron travels some finite distance from the electrode surface before reacting with the oxidized species. On the basis of measurements in related

liquids, we would estimate the thermalization distance in MeCN to be about 3–5 nm.<sup>38</sup> An alternative possibility would be direct reaction of a conduction band electron with a specifically adsorbed oxidant to form an adsorbed excited state. In this case, the formation of a hot electron in the solution phase would not be invoked. However, there is no evidence that these ions are specifically adsorbed from MeCN solutions, and the fact that addition of a Pt layer increases the emission<sup>34</sup> suggests that a solution process is more likely. Experiments are underway in an attempt to probe these alternative paths.<sup>39</sup>

The question also arises whether the hot electrons injected into solution form a solvated electron before reaction with the acceptor molecule. This question has been raised in connection with injection in aqueous media from an Al/Al<sub>2</sub>O<sub>3</sub> electrode.<sup>40</sup> While it has been established that ECL can be produced from solvated electrons in liquid ammonia, a medium in which they are stable,<sup>41</sup> there is no evidence for the intermediacy of these in MeCN. In fact, the energy needed to produce a solvated electron in MeCN would be at the background reduction of the solvent and at much more negative potentials than those needed to generate the ECL observed here. Thus, the mechanism we favor is direct reaction of hot electrons at or near the electrode surface to form excited states without the intermediacy of a solvated electron.

Finally, one should contrast the ECL emission seen here, clearly consistent both electrochemically and spectrally with production of the excited state by an electron-transfer reaction, with other processes that can lead to light emission. For example, with large applied voltages (e.g.,  $|V| > 10$  V) and current densities, electroluminescence of oxide films, including Ta<sub>2</sub>O<sub>5</sub>, can be observed. Other types of emission, e.g., of hot electrons interacting with thin metal films or cathodoluminescence are also possible but should not be observed under the conditions of these experiments.

## Conclusions

Injection to produce hot electrons in a solution to form directly excited states has been established by the reduction of TH<sup>+</sup> and HMC<sup>2+</sup> at a Ta<sub>2</sub>O<sub>5</sub>-coated Ta electrode. This result conforms to a model in which the energy levels in the oxide and solution have been estimated by electrochemical measurements and electrons are injected via the conduction band of the Ta<sub>2</sub>O<sub>5</sub>. Electrochemical generation of hot electrons to produce products not available with thermal electrons injected from a metal like Pt would be of interest. However, higher efficiency of hot electron injection is needed before these types of experiments are undertaken. It is also of interest to study the effect of the solvent and electrode material on hot-electron processes. The analogous oxidation process in which hot holes are injected via the valence band of a wide band gap material would also be interesting.

**Acknowledgment.** The support of this research by the National Science Foundation (CHE9423874) and the Robert A. Welch Foundation is gratefully acknowledged. We are indebted to Drs. Art Nozik and Cynthia Zoski and the reviewers for their helpful comments.

## References and Notes

- (1) Schmidt, W. F. *Liquid-State Electronics of Insulating Liquids*; CRC Press: Boca Raton, FL, 1997; p 260.
- (2) Morrison, S. R. *Electrochemistry at Semiconductor and Oxidized Metal Electrodes*; Plenum Press: New York, 1980; p 350, et seq.
- (3) Cavanagh, R. R.; King, D. S.; Stephenson, J. C.; Heinz, T. F. *J. Phys. Chem.* **1993**, *97*, 786.

- (4) Gurevich, Y. Y.; Pleskov, Y. V.; Rotenberg, Z. A. *Photoelectrochemistry*; Consultants Bureau: New York, 1980.
- (5) Krivenko, A. G.; Krüger, J.; Kautek, W.; Benderskii, V. A. *Ber. Bunsen-Ges. Phys. Chem.* **1995**, *99*, 1489 and references therein.
- (6) Cooper, G.; Turner, J. A.; Parkinson, B. A.; Nozik, A. J. *J. Appl. Phys.* **1983**, *51*, 6463.
- (7) Koval, C. A.; Howard, J. N. *Chem. Rev.* **1992**, *92*, 411.
- (8) Nozik, A. J.; Memming, R. *J. Phys. Chem.* **1996**, *100*, 13061.
- (9) Groner, M. D.; Watts, D. K.; Koval, C. A. *J. Electrochem. Soc.* **1997**, *144*, 1690.
- (10) Diesing, D.; Rüsse, S.; Otto, A.; Lohrengel, M. M. *Ber. Bunsen-Ges. Phys. Chem.* **1995**, *99*, 1402.
- (11) Chen, C.; Frese, K. W. *J. Electrochem. Soc.* **1992**, *139*, 3243 and references therein.
- (12) (a) White, H. S.; Bard, A. J. *J. Am. Chem. Soc.* **1982**, *104*, 6891. (b) Becker, W. G.; Seung, H. S.; Bard, A. J. *J. Electroanal. Chem.* **1984**, *167*, 127.
- (13) Kulmala, S.; Ala-Kleme, T.; Heikkilä, L.; Väre, L. *J. Chem. Soc., Faraday Trans.* **1997**, *93*, 3107 and references therein.
- (14) (a) Yeh, L. R.; Bard, A. J. *Chem. Phys. Lett.* **1976**, *44*, 339. (b) Luttmmer, J. D.; Bard, A. J. *J. Electrochem. Soc.* **1978**, *125*, 1423.
- (15) Gleria, M.; Memming, R. *Z. Phys. Chem.* **1976**, *101*, 171.
- (16) Grabner, E. W. *Electrochim. Acta* **1975**, *20*, 7.
- (17) Brilmyer, G.; Bard, A. J. *J. Electrochem. Soc.* **1980**, *127*, 104.
- (18) Bard, A. J.; Faulkner, L. R. *Electrochemical Methods*; Wiley: New York, 1980; p 701.
- (19) Lee, S. K.; Richter, M. M.; Stekowski, L.; Bard, A. J. *Anal. Chem.* **1997**, *69*, 4126.
- (20) Schmickler, W.; Schultze, J. W. In *Modern Aspects of Electrochemistry*; Bockris, M. O'M., Conway, B. E., White, R. E., Eds.; Plenum Press: New York, 1986; Vol. 17, p 357.
- (21) Clechet, P.; Martin, J.-R.; Olier, R.; Vallony, M. C. *C. R. Acad. Sci.* **1976**, *282*, 887.
- (22) Frank, S. N.; Bard, A. J. *J. Am. Chem. Soc.* **1975**, *97*, 7427.
- (23) Keszthelyi, C. P.; Tokel-Takvoryan, N. E.; Bard, A. J. *Anal. Chem.* **1975**, *47*, 249.
- (24) Ouyang, J.; Bard, A. J. *J. Electroanal. Chem.* **1987**, *222*, 331.
- (25) Sung, Y.-E.; Bard, A. J. Unpublished experiments.
- (26) Tokel-Takvoryan, N. E.; Hemingway, R. E.; Bard, A. J. *J. Am. Chem. Soc.* **1973**, *95*, 6582.
- (27) Laser, D.; Bard, A. J. *J. Electrochem. Soc.* **1975**, *122*, 632.
- (28) (a) Wallace, W. L.; Bard, A. J. *J. Phys. Chem.* **1979**, *83*, 1350. (b) Glass, R. S.; Faulkner, L. R. *J. Phys. Chem.* **1981**, *85*, 1159.
- (29) Morrison, S. R. *Electrochemistry at Semiconductor and Oxidized Metal Electrodes*; Plenum Press: New York, 1980; pp 315–331.
- (30) (a) Vijn, A. K. *Electrochemistry of Metals and Semiconductors*; Marcel Dekker: New York, 1973. (b) Young, L. *Anodic Oxide Films*; Academic Press: New York, 1961.
- (31) (a) Schmickler, W. *Ber. Bunsen-Ges. Phys. Chem.* **1978**, *82*, 477. (b) Schmickler, W.; Ulstrup, J. *Chem. Phys.* **1977**, *19*, 217.
- (32) Yoneyama, H.; Ochi, K.; Tamura, H. *J. Appl. Electrochem.* **1976**, *6*, 283. (b) Randall, J. J.; Bernard, W. J.; Wilinson, R. R. *Electrochim. Acta* **1965**, *10*, 183.
- (33) Moses, P. R.; Wier, L. M.; Lennox, J. C.; Finklea, H. O.; Lenhard, J. R.; Murray, R. W. *Anal. Chem.* **1978**, *50*, 576.
- (34) Sung, Y.-E.; Bard, A. J. *J. Phys. Chem.* **1998**, *102*, 9806.
- (35) Mead, C. A. *Phys. Rev.* **1962**, *128*, 2088.
- (36) *Scanning Tunneling Microscopy and Spectroscopy*; Bonnell, D. A., Ed.; VCH: New York, 1993; p 9.
- (37) Zhang, X.; Bard, A. J. *J. Am. Chem. Soc.* **1988**, *92*, 5566.
- (38) *Kinetics of Nonhomogeneous Processes*; Freeman, G. R., Ed.; J. Wiley: New York, 1987; Chapter 2.
- (39) The definition of Fermi level in the liquid phase, and hence the energy of a thermal electron, is almost always based on the electrochemical potential of an electron in equilibrium and strongly associated with a redox couple. For example, in the thianthrene solution, the Fermi level is governed by the E<sup>0</sup> and concentrations of TH<sup>+</sup> and TH. Only for solutions in which electrons have reasonable stability, such as liquid NH<sub>3</sub>, would a thermal electron be identified as an actual electron concentration, and even here, the electron interacts strongly with the solvent and counterions (e.g., K<sup>+</sup>). In an analogous way, one might then adopt the concept of a hot electron as one that is strongly associated with a molecule, e.g., an excited state. However, this definition would broaden the concept well beyond that usually implied by hot electrons in a liquid phase weakly interacting with solvent.<sup>1,38</sup>
- (40) (a) Kulmala, S.; Ala-Kleme, T. *Ber. Bunsen-Ges. Phys. Chem.* **1997**, *101*, 758. (b) Diesing, D.; Krizler, G.; Otto, A. *Ber. Bunsen-Ges. Phys. Chem.* **1997**, *101*, 762.
- (41) Itaya, K.; Bard, A. J. *J. Phys. Chem.* **1981**, *85*, 1358.